

Using Road Surface Measurements for Real Time Driving Simulation

Ben G. Kao and Bruce Artz
Ford Research Laboratories
Ford Motor Company
Dearborn, Michigan 48121-2053

ABSTRACT

Road surface irregularity is known to effect vehicle NVH responses. When modeling vehicle NVH, it is desirable to have high-resolution measurements of the road surface to use as road input. For typical NVH modal tire models, the road surface sampling rate will not be an issue because several points on the tire patch (center line) are used to determine the road surface irregularity. The single point follower tire model, often used in real time driving simulation, uses only one point to establish the tire patch. In this case, the sampling interval of the road surface can effect the resulting excitation of vehicle vibrations.

In this paper, measured road surfaces are studied in terms of the vehicle dynamic point follower tire model. Among the issues to be discussed are: the vehicle speed, the tire patch length, the road surface sampling rate and averaging procedures. In this study, a procedure to define the road roughness surfaces usable for driving simulations will be identified. A vehicle model is used to validate the procedure through comparisons with vehicle measured vibration data.

Email Addresses:

Ben Kao bkao@ford.com
Bruce Artz: bartz@ford.com

INTRODUCTION

Road surface modeling for real time driving simulations depends on the simulator characteristics and the purpose of the simulations. Climbing up a curb-island is used for road load simulations but is not necessary for the high-speed freeway driving unless a special study is intended. For the curb-island event, if a driving simulation is really intended, it is necessary to separate the tire tread and the sidewalls so both enveloping and tire dynamics can be considered [1]. Driving simulation, at the Ford Motor Company driving simulator (VIRTTEX), is primarily concerned with normal highway driving which does not involve such road irregularities. Approaches, such as that adopted by Turpin, are therefore not necessary [2]. VIRTTEX is primarily concerned with normal NVH and handling responses. Consequently, road surfaces for the driving simulations with VIRTTEX are more representative of the regular freeway surfaces or rough road of random irregularities but without drastic sharp and severe discontinuities.

All road surfaces are made to be not perfectly flat for the required road friction so safe driving will be possible. But the road surface irregularities also cause the vibrations of the suspensions and the vehicle body. To the drivers and the passengers such vibrations cause the sensation of ride and affect comfort. This paper is concerned with the use of existing road surface data for reasonable driving simulation feed back.

THE VEHICLE DYNAMICS MODEL

The vehicle dynamics model used in this study is an improved version of the model from Greenberg and Park [3], which has 1 degree of freedom for each suspension. The model used in this study separated the engine mass and front sub-frame mass from the vehicle body for the purpose of improving vehicle resonance frequency predictions. The relevant information for the vehicle model is given in Table 1:

Body mass (Kg)	1011.31
Engine (Kg)	304.4
Subframe (Kg)	24.57
Driver & Passenger (Kg)	147
Front Unsprung mass (Kg)	42.39
Rear Unsprung mass (Kg)	31.24
Wheel base (M)	2.76
Front track width (M)	1.556
Rear track width (M)	1.569

Table 1: Basic vehicle data.

The spring rates for the vehicle are 2.15×10^4 N/M for the front and 1.75×10^4 N/M for the rear. The shock characteristics are approximated by 3rd order polynomials instead of straight lines (Greenberg and Park [3]). The front shock curve is approximated by equation (1).

$$\begin{aligned} F_J &= 2141 \cdot V - 2392 \cdot V^2 + 1134.4 \cdot V^3 \\ F_R &= 4484.6 \cdot V + 4039.2 \cdot V^2 + 1650 \cdot V^3 \end{aligned} \quad (1)$$

The polynomial fit and shock design data are compared in Figure 1. The positive shock velocity (M/sec) is for the jounce velocity. Since no sharp ground discontinuity such as a chuckhole is involved in the

simulations, the shock speeds outside the test data range are rarely reached in the simulations. The monotonically increasing slope of the shock curve in the whole range of shock speed guarantees the stability of the shock model in the simulations. Similarly, the rear shock curve is approximated by equation (2).

$$\begin{aligned} F_J &= 1470 \cdot V - 1573.6 \cdot V^2 + 775.7 \cdot V^3 \\ F_R &= 2578 \cdot V + 2754.6 \cdot V^2 + 1453.1 \cdot V^3 \end{aligned} \quad (2)$$

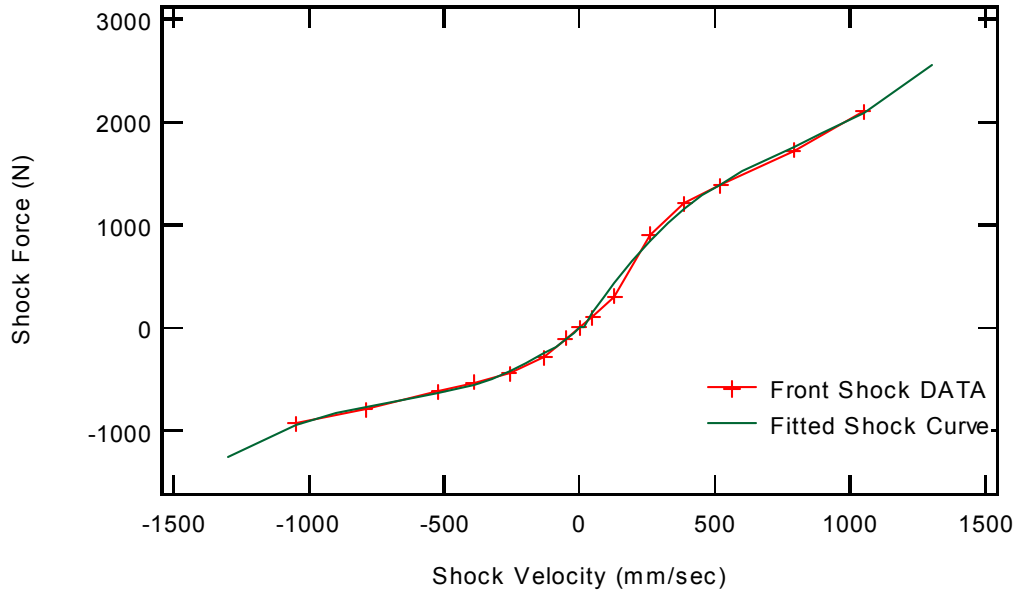


Figure 1: The shock curve for the front suspension.

The aerodynamic forces on the vehicle are also included in the vehicle model as described in [3]. The vehicle model has been validated with vehicle test data for body roll angle, pitch angle, understeer gradient, etc. so the behavior of the vehicle model is representative of the vehicle. The engine added has six degrees of freedom but the sub-frame has only three linear degrees of freedom in the model. This is sufficient for this study since only vertical vibration of the vehicle system is considered in this study. A separate simulation with all six degrees of freedom of the subframe confirmed this assessment. Thus the final vehicle dynamic model used for this study has a total of 19 degrees of freedom. (Not counting the tire model degrees of freedom.)

TIRE PATCH POSITION

The effect of the road on the tire forces is determined by the road surface height, the orientation of the surface normal, the wheel camber angle and the wheel load. Figure 2 is a head on, front view of the tire ground interface showing all the relevant kinematical quantities in the SAE vehicle dynamic coordinate system [7]. It consists of the plane formed by the vectors of the surface normal \mathbf{n} and the wheel spin axis \mathbf{s} . \mathbf{W}_c is the position vector of the wheel center and \mathbf{T}_c is the largest penetration of the tire center into the ground surface as if the surface did not present any resistance to the tire patch. For further understanding of Figure 2, we note also that the tire velocity vector \mathbf{u}_x , which is parallel to the road surface, is normal to and coming out of the plane. The vector \mathbf{t} , which is in the plane, is normal to \mathbf{s} , and points from the wheel center to contact patch center (co-linear with $\mathbf{W}_c - \mathbf{T}_c$ line). The vectors \mathbf{n} , \mathbf{s} and \mathbf{t} are all normalized unit vectors for the discussions that follow. We should also note that the gravitational direction vector \mathbf{k} is not shown in Figure 2 since it is in general not in this plane unless the velocity vector \mathbf{u}_x is horizontal. This figure helps to find the magnitude of the tire normal deflection (ΔR) and hence to define the tire radial force (which is a function of tire deflection).

In order to define all the vectors consistently, the unit vectors \mathbf{n} and \mathbf{s} are used. First, the unit vector of the wheel ground velocity is defined, as shown in Figure 2 and explained earlier:

$$\mathbf{u}_x = \frac{\mathbf{s} \times \mathbf{n}}{|\mathbf{s} \times \mathbf{n}|} \quad (3)$$

The position vector \mathbf{T}_c under the assumption that the tire circle remains circular then determines the tire disc's largest penetration point.

$$\mathbf{T}_c = \mathbf{W}_c + R \mathbf{t} \quad (4)$$

\mathbf{W}_c is the wheel center position vector determined through vehicle position, the scalar R is the known undeformed tire radius and \mathbf{t} is a unit vector in the same plane determined by equation (5).

$$\mathbf{t} = \mathbf{u}_x \times \mathbf{s} \quad (5)$$

Using the ground surface height data and the position of \mathbf{T}_c , the tire patch center position \mathbf{P} and tire deflection Δz can be determined. The tire deflection at the tire patch center, ΔR , can be approximated by,

$$\Delta R = \Delta z \mathbf{n} \cdot \mathbf{k} / \mathbf{n} \cdot \mathbf{t} \quad (6)$$

where, Δz is measured in the direction of gravity \mathbf{k} (see Figure 2 and note that the definition of the surface height is in the \mathbf{k} direction).

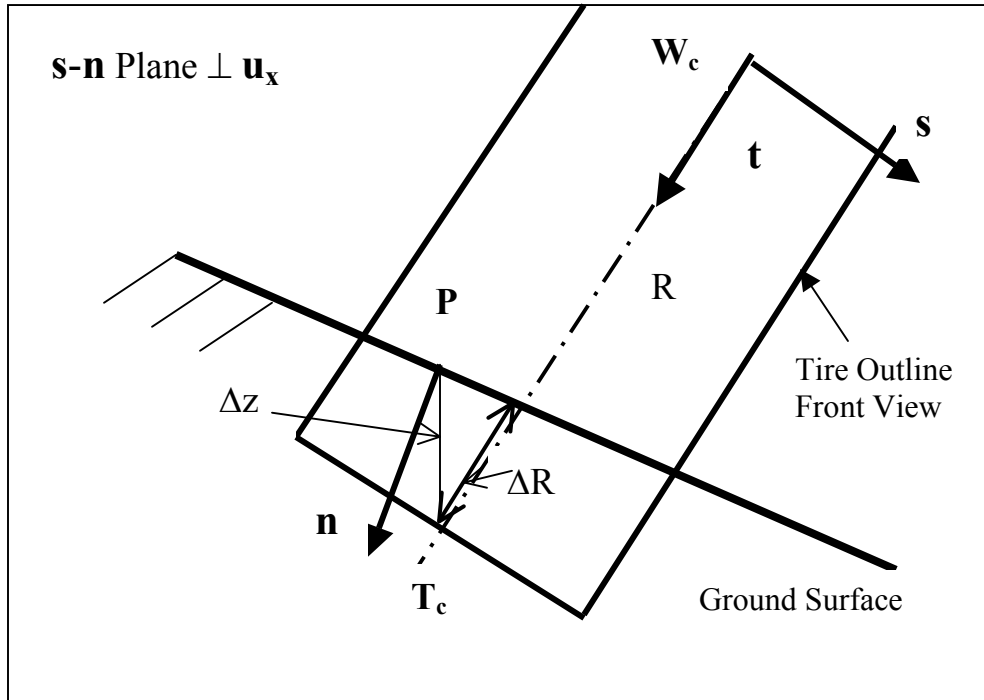


Figure 2: Tire/Ground relationship in a front view during a simulation.

Figure 2 also shows that this approach does not provide the exact tire patch center position when a non-zero wheel to ground camber angle exists. That is, the position \mathbf{P} is not located at the tire patch center in general. However, the surface normal at \mathbf{P} and the resulting tire deflection ΔR can be used if the ground does not include a sudden profile change in the neighborhood of \mathbf{P} (as shown in the figure). Furthermore, in the real time simulation, the ground surface information of the previous time step is used to estimate the

current tire patch position. Consequently, equation (6) is an acceptable approximation unless a sharp edged ground surface is involved in the simulation. In practice, however, the deformed tire radius is used in the vehicle dynamic model because \mathbf{P} is only used to calculate ΔR .

The value of tire deflection ΔR is then used to calculate the normal force. The triad made of vectors \mathbf{n} and \mathbf{u}_x and another unit-vector \mathbf{u}_y perpendicular to both of them (and hence parallel to the ground surface) are used for ground surface forces calculations and application. This triad aligns itself with the tire patch.

For real time simulations this tire triad is not available until the surface normal is known. On the other hand, the surface normal is known only after the tire patch position is determined. Since the iteration to get the converged solution is not feasible in real time simulation, results of the previous time step is kept to initiate the calculation of the new tire patch position \mathbf{P} and surface normal \mathbf{n} . Then \mathbf{t} , \mathbf{u}_x , \mathbf{u}_y and tire patch center are all updated for current step before proceeding to the full calculation. It is also assumed that at the initiation of the simulation ($t = 0$) the ground surface height is zero and horizontal (\mathbf{n} is in the direction of \mathbf{k}).

With \mathbf{t} , \mathbf{u}_x and \mathbf{n} known, it will be possible to calculate the wheel camber angle which is then used for tire force and moment calculations. The updated wheel information is used for all the tire patch calculations explained here. In this paper, since the simulations are for the vehicle driving straight, the steering motion for the calculation of the wheel center position and the wheel orientation change are not applied. However, the wheel camber changes due to spindle motion and ground normal \mathbf{n} are included.

THE TIRE PATCH LENGTH

The tire model used in this study is a modified form of the Pacejka Magic Formula [5]. It is a point follower force model, represented by the tire patch position and by a single deformed tire radius. The tire patch length for any given tire load can be measured from a tire test or calculated using a finite element model of the particular tire. Using a finite element analysis of the tire, the tire patch length for the front tire is calculated to be 169mm (load 5120N) and rear tire to be 136mm (load 3500N). Though the tire loads are not constant in the driving conditions, since our simulation is in a straight line for vehicle vertical vibrations, the variation of tire patch length is overlooked. For simplicity of analysis, it is further assumed that the tire patch length for the front and rear has the same length 150mm. This could cause a difference in the number of road data points for averaging the tire patch height and the normal direction. For 169 mm patch the number of road profile points is about 34 while 150 mm patch is about 31 (road profile data have 5mm interval between consecutive patch points). But it will become clear in later discussion that this difference will not cause significant changes in vehicle vibration characteristics.

PREPARATION OF ROAD SURFACE PROFILE DATA

Road surface profile data are available for several Ford Motor Company test tracks. Originally, these profiles were measured for vehicle NVH (noise, vibration and harshness) studies. Vehicle NVH studies are usually not concerned with the low frequency vehicle response below 5 Hz. A high pass filter is applied to eliminate the frequencies below 5 Hz before these data are used for NVH simulations. For driving simulation, however, frequencies down to about 0.5Hz significantly relate to the senses of the driver and passengers. We have selected two roads for which vibration data were available for the particular vehicle we modeled. One road was very smooth and the other rough.

These high-resolution road profiles are obtained using a specially equipped conventional sedan. This vehicle has 2 laser displacement sensors and 2 accelerometers, capable of DC measurements, mounted at the rear bumper mounts so that they follow the rear wheels. A non-contact speed sensor is also used. Figure 3 shows this equipment. The vehicle is driven slowly (~ 2 m/s) and data is sampled at 6000 Hz. The accelerometer data is double integrated to obtain the vertical motion of the vehicle, which is then subtracted from the laser displacement data. The spatial domain data is then sub-sampled giving data at the desired spacing.



Figure 3. Laser displacement sensors, accelerometers, and non-contact speed sensor used to obtain road profiles.

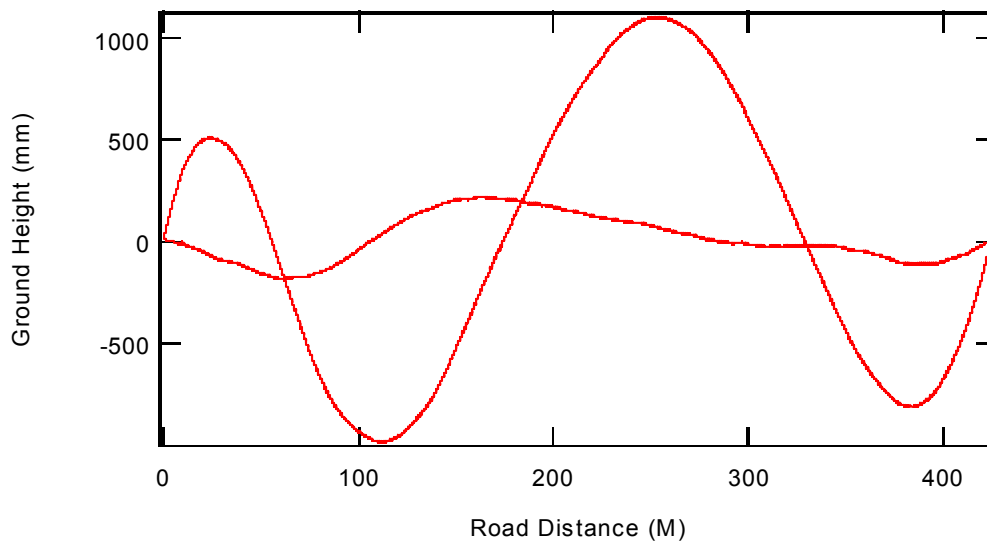


Figure 4: Road profiles of the smooth road raw data.

Smooth Road Profiles

The left and right track raw road surface profiles for the smooth track are plotted in Figure 4. It is clear that the road profiles contain substantial measurement drifts. We shall note that the significant road profile fluctuations are entirely contained in the thickness of the curves: the large drifts completely mask the small

fluctuations in the data. This data cannot be applied to the vehicle directly because of the differences between the drifts on each track. The data must be high pass filtered first. The high pass filter should be chosen to eliminate the instrumental drift but to keep as much low frequency data as possible. Spatial high pass filters of 0.025 cyc-m^{-1} , 0.05 cyc-m^{-1} and 0.125 cyc-m^{-1} were tried.

As an example, the pair of the profiles filtered with the 0.025 cyc-m^{-1} filter are shown in Figure 5. Using a vehicle speed of 48 KPH (30 MPH) the power spectral densities for the filtered road profiles, are shown in Figure 6. For this speed, the road profiles processed with 0.025 cyc-m^{-1} and 0.05 cyc-m^{-1} filters are very similar. However, the 0.125 cyc-m^{-1} filter reduced significantly the road profile frequency content below 2 Hz.

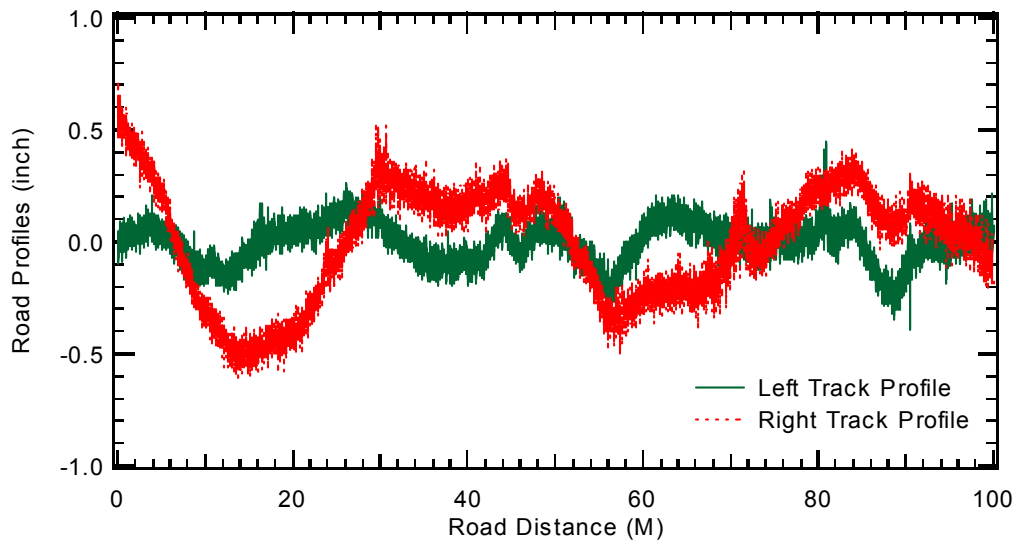


Figure 5: The filtered road profiles used for vehicle model simulations.

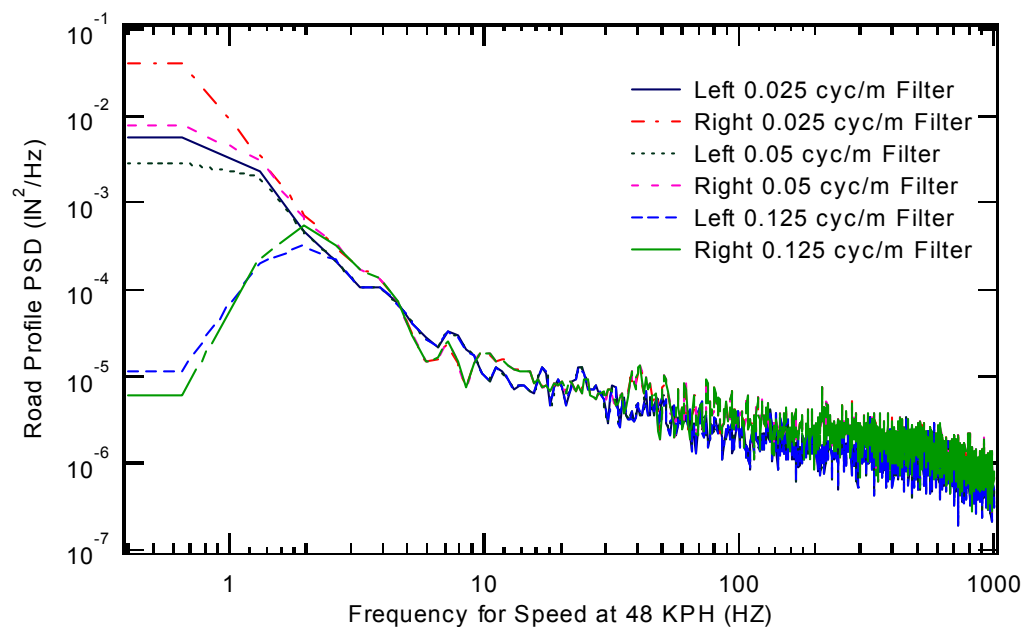


Figure 6: PSD analyses of the smooth road profiles after high pass filters.

Rough Road Profiles

The raw rough road profiles are shown in Figure 7 exhibiting similar drift characteristics. The power spectral density analyses of these profiles, based on the 64KPH (40MPH) speed, are shown in Figure 8. Only 0.05 cyc-m⁻¹ and 0.125 cyc-m⁻¹ filters were used. Both filters show acceptable road roughness frequency content down to 0.5 Hz. At this speed, the 0.025 cyc-m⁻¹ filter did not entirely remove the instrumental drift.

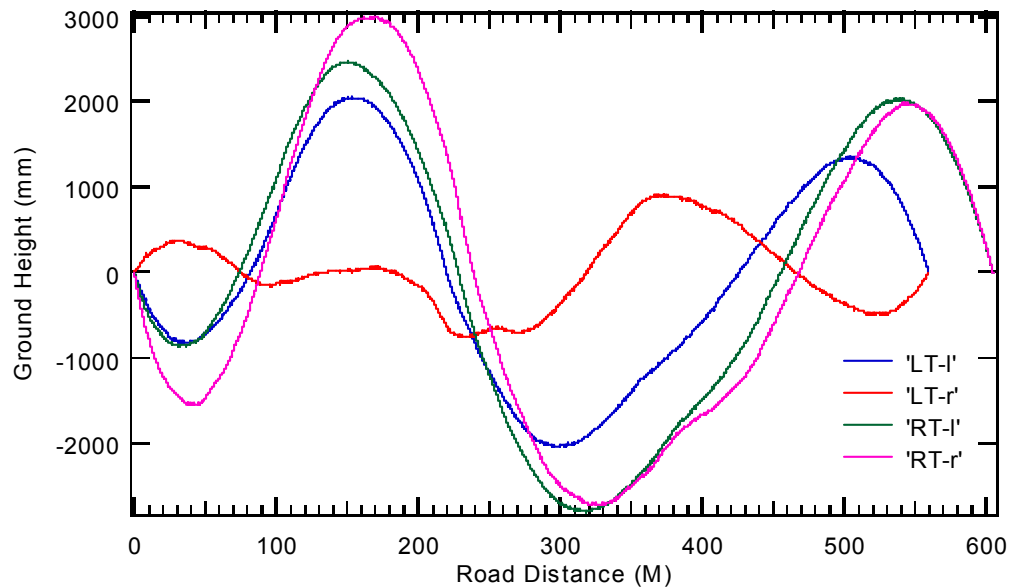


Figure 7: Raw data from the road profiles measured for vehicle NVH simulations.

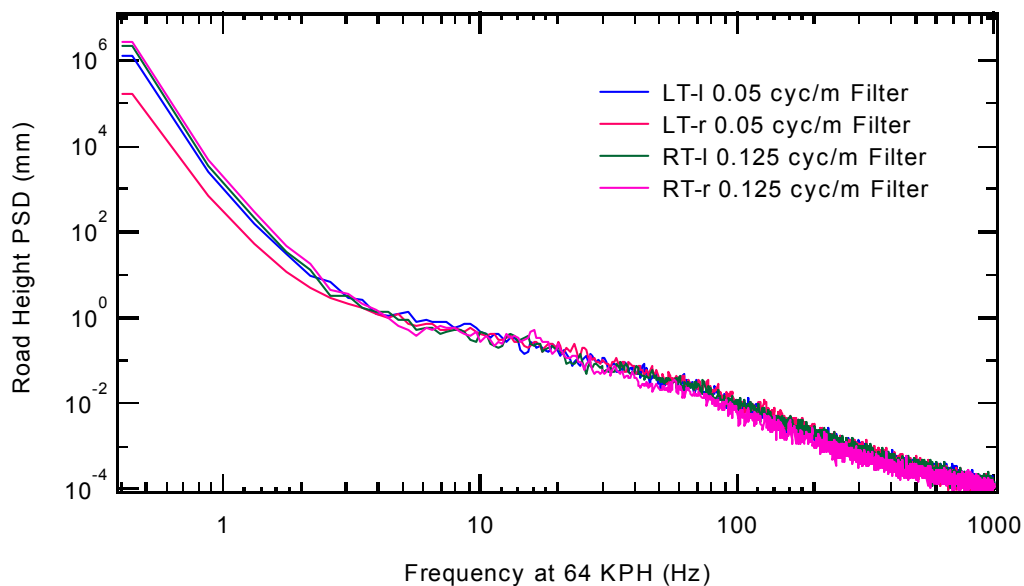


Figure 8: Power Spectral Densities of the road profiles with vehicle speed at 64 KPH. Note the frequency content flat out below about 0.45 Hz.

Road Profile Presentation

The road profile data is stored in the vehicle simulation program. When the vehicle exceeds the limit of the available road profile, the profiles are reflected and repeated. This ensures a road surface without any artificial discontinuities that maintains the same PSD.

Determination of Road Height and Surface Normal Direction

At 48 KPH, the vehicle simulation program samples the road profile about every 17 mm. The road surface height and normal used in the simulation are calculated using a least square linear fit to the road heights of all the points falling within the 150mm of the tire patch length. The road height is the average height of the points and the surface normal is in the direction perpendicular to the line. This approach takes into consideration tire averaging (enveloping) of the road profiles. It will be demonstrated that this approach for the 5mm sampling distance road data correlates well with test results. Same approach is used for the 64 KPH simulations.

SMOOTH ROAD RESULTS

Filtering and Speed Effects

Simulation vertical acceleration results at the driver left front seat track of the vehicle model at 48 KPH are compared with measured data from a test vehicle in Figure 9. We see that the 0.125 cyc-m⁻¹ high filter eliminated most vehicle responses below 1.5Hz while the 0.05 cyc-m⁻¹ and 0.025 cyc-m⁻¹ filters result in very similar vehicle responses and the predictions are reasonable for frequencies below 1Hz. This agrees with the road profiles PSD results as shown in Figure 6. The comparison with test data also reveals that the road profiles used in the simulation might contain results of measurement drift as shown by the extra resonance observed near 0.7Hz. In general, the 0.05 cyc-m⁻¹ high filter is a reasonable choice based on the comparison shown in Figure 9.

Above 1.5 Hz the model frequency responses are almost the same for all filters. The predictions are reasonable for the wheel hop mode (~13 Hz). The nearly flat response as shown in test data between 3.5 Hz and 6 Hz is not reproduced in the model. For frequencies above 12 Hz, the model becomes under-predicting. The limited degrees of freedom in the vehicle model and the single spring tire model contribute to this effect. The resonance at 90Hz as shown in the test data will be discussed in the discussion for the rough road later.

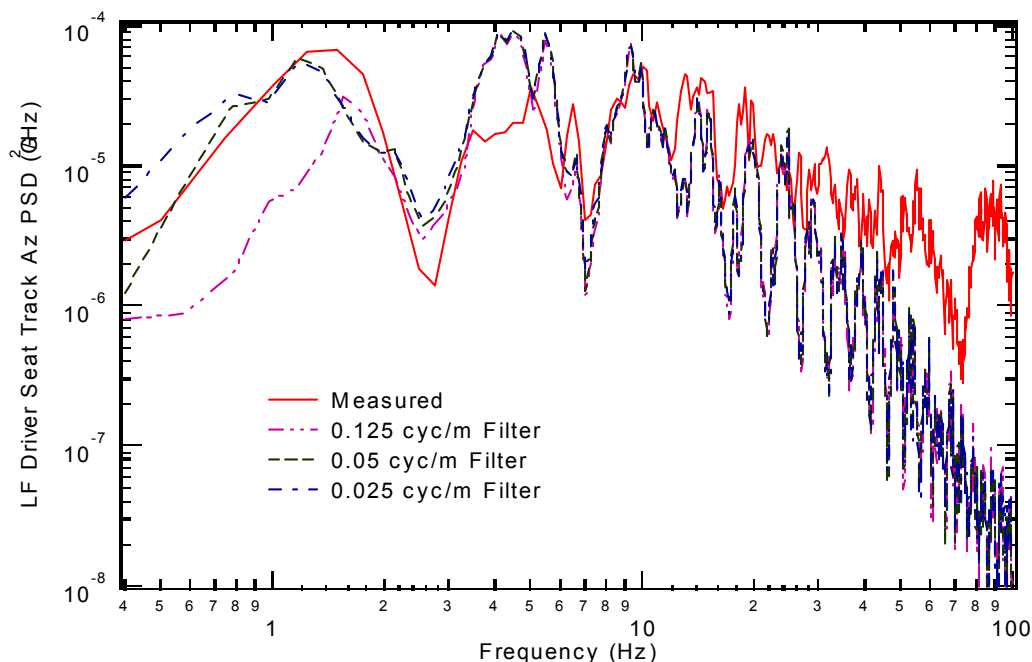


Figure 9: Comparisons for different road profile filters.

The vehicle simulation was also run at 64 KPH (40 mph) using the 0.05 m^{-1} filtered road surface. The results are shown in the blue line in Figure 10 to compare with the test data and the 48KPH results. As expected, the vehicle responses are shifted to higher frequencies since the road input frequencies are shifted upward. These results also confirm that the 48KPH simulation speed is a reasonable representation of the vehicle speed during measurement, which might involve slight speed deviation.

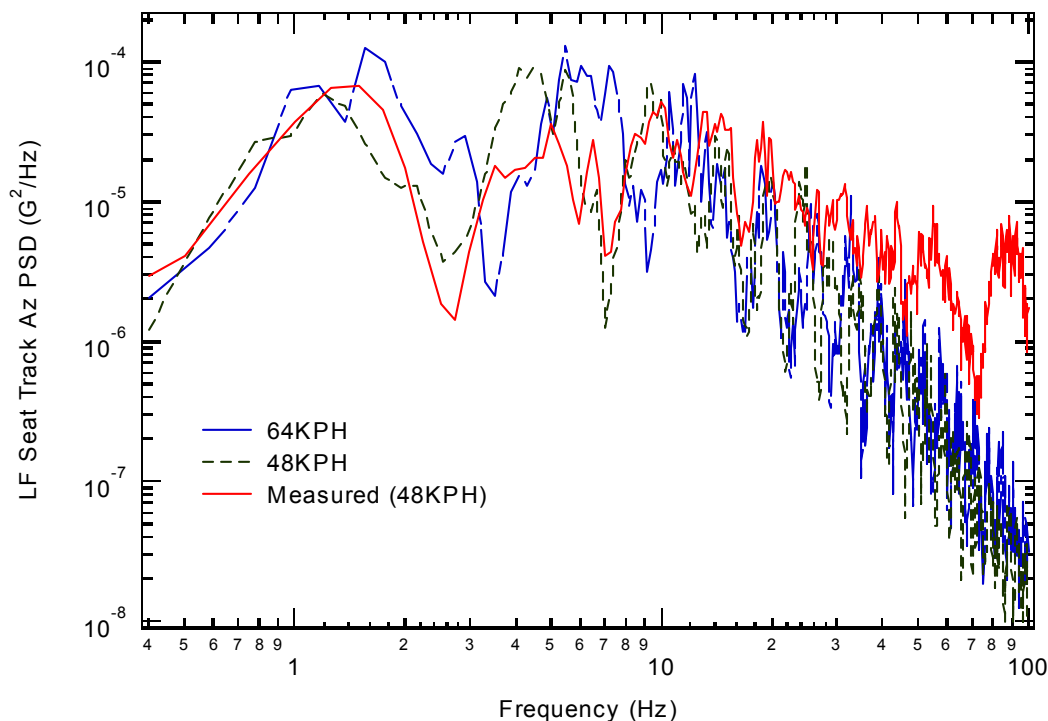


Figure 10: Comparison of the vehicle model driving on the same road profile with higher vehicle speed (64KPH) than the test vehicle speed (48KPH).

Effect of Road Profile Sampling Distance

Many road profiles are not as refined as the data created for NVH simulations. Road profiles having a sampling distance of about 152.4mm (6 inches) are common. To investigate the effect of sampling distance on the simulation the 0.05 cyc-m^{-1} filtered road profiles were sub-sampled creating road profiles with 75mm and 150mm sampling distances. Figure 11 compares simulations run on these profiles with the previous results. The same method for determining road height and normal direction were used. For frequencies below 7 Hz there is very little difference.

For easier comparison, the results shown in Figure 11 are re-plotted in Figure 12 in frequency range between 5 and 50 Hz. From 6 to 16 Hz both 75mm and 150mm road sampling distances yield vibration amplitudes higher than that of the 5mm sampling distance. Above 16 Hz the 5mm data falls between the 150mm and 75 mm data. We believe the 5mm sampling represents the most realistic result when using the linear least squares method. The fact that the 75mm and 150mm sampling shows no trends indicates that this method of determining the road height and normal direction is inappropriate for these data.

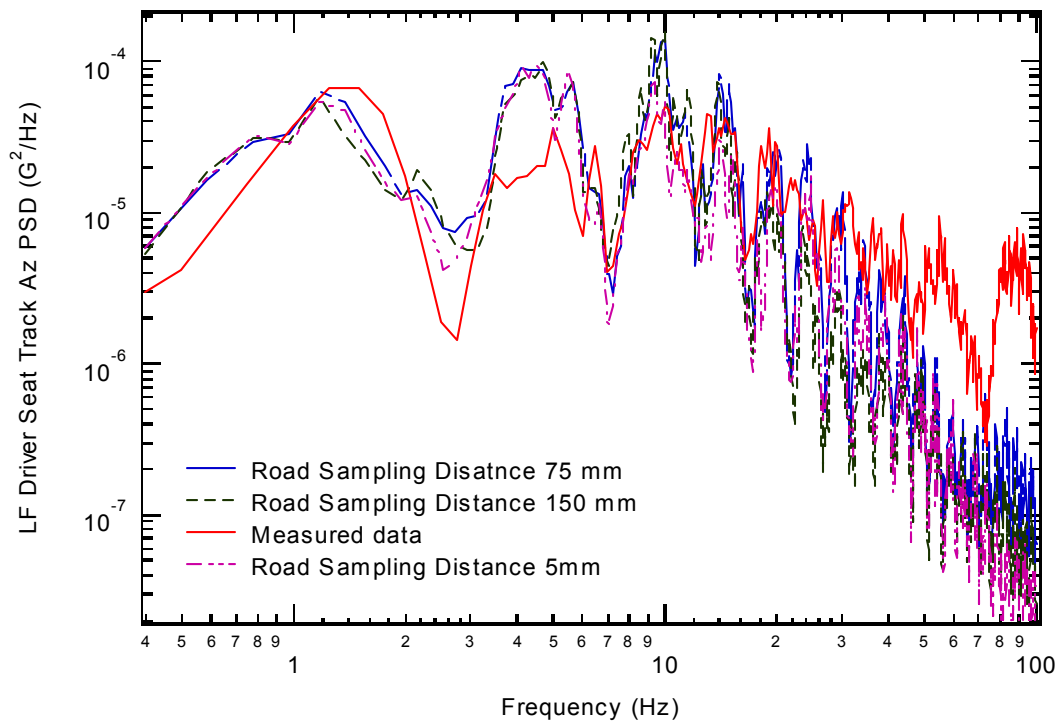


Figure 11: Comparison for the road sampling distances.

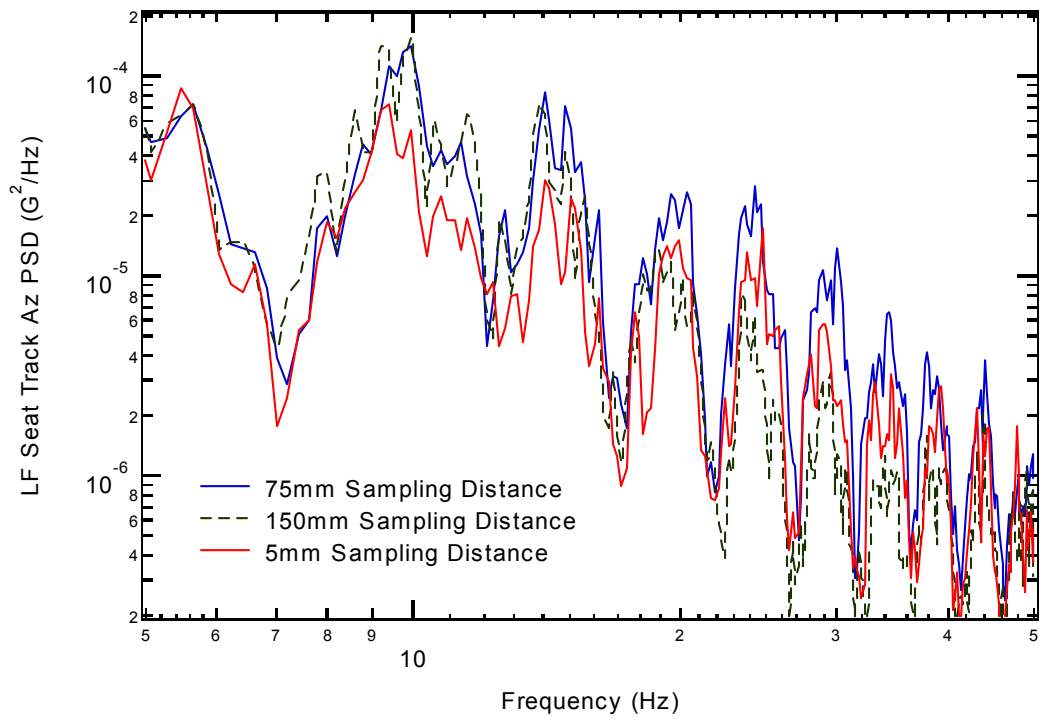


Figure 12: Simulation results for different sampling distances between 5 and 50Hz.

When using the road profiles measured at 6 inches intervals, a different road profile treatment is needed. A curve fitting process can be used instead of least square linear fitting. A third order polynomial is fitted to the 4 points nearest to the tire patch center, and it is used to calculate the ground height and the ground normal (normal to the curve) at the patch center. This process yields a different approximation for the road surface, which has similar height but higher normal variations (Table 2). The vehicle simulation results are shown in Figure 13. This shows that the curve fitting process gives a similar response to the least squares linear method for frequencies below 17Hz but gives higher response for higher frequencies. For the data with sampling distance near 150mm the curve fitting method seems is a better approach if the response information over 17Hz is needed for driver feed back. Otherwise, the linear least square method will provide sufficient responses. Nevertheless, the refined surface data is still a better approximation for it is the more realistic response based on the comparison up to frequency 20 Hz.

	Left		Right	
	$\sigma_{Z(m)}$	σ_{N_x}	$\sigma_{Z(m)}$	σ_{N_x}
LLSQ	0.00215	0.00464	0.00632	0.00563
3 rd Poly	0.00220	0.00534	0.00631	0.00632

Table 2: Standard deviations of surface height (σ_Z) and surface normal in the x-direction (σ_{N_x}). LLSQ uses the linear least square method to determine Z and N while 3rd Poly uses the 3rd order polynomial fit. The surface used has been sub-sampled to 150 mm. The maximum height deviation is about 2% but the deviations for N_x on the left tires is 15% and on the right tires is 12%.

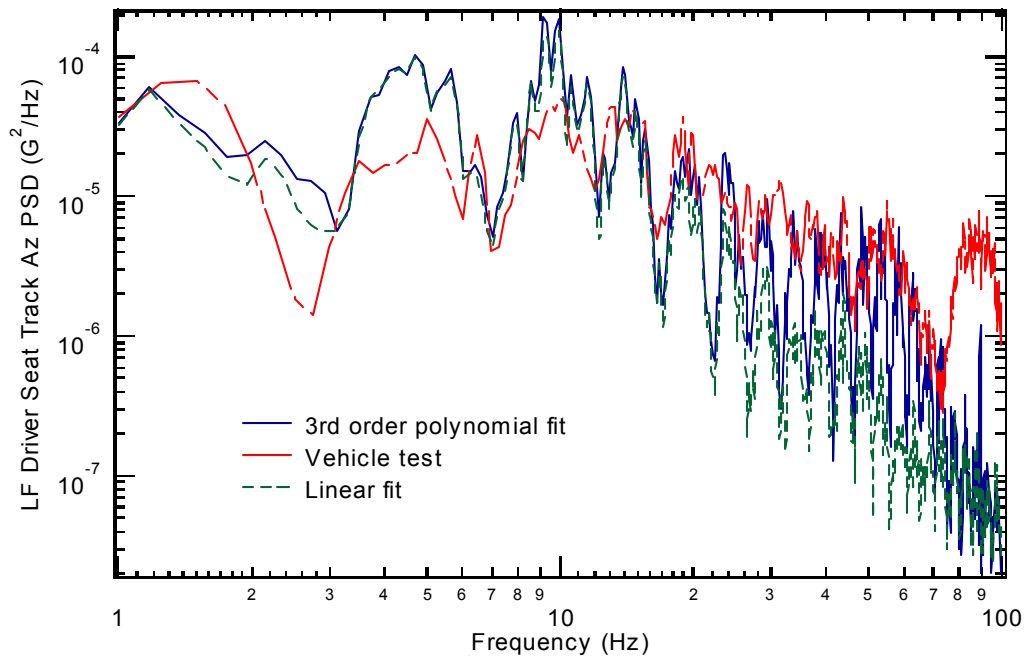


Figure 13: Comparison of using 3rd order polynomial fit for the road surface 150mm sampled data.

Further investigation with the normal vector fixed in vertical direction (150mm sampling distance) shows that the vertical vibration is almost identical to the case using the normal direction provided by the polynomial. This demonstrated that for the 150mm sampling distance the increase of the vibration amplitudes is caused by the increase of the ground height variation. The deviation of ground normal in the x-direction is too small for the normal vector. The predicted difference between the 75 mm sampling distance and 150 mm ground sampling distances, however, is primarily caused by the difference in the normal direction. For the ground surface data with 6 inches sampling distance of a smooth road, therefore, the polynomial fit is the better approximation, with or without local tangent determined normal direction.

ROUGH ROAD RESULTS

Vehicle simulations were run at 64KPH using the same vehicle model and 0.125 cyc-m^{-1} and 0.05 cyc-m^{-1} high pass filtered rough road profiles. Figure 14 shows the results with the field measured vehicle acceleration data for the driver's left-front seat track.

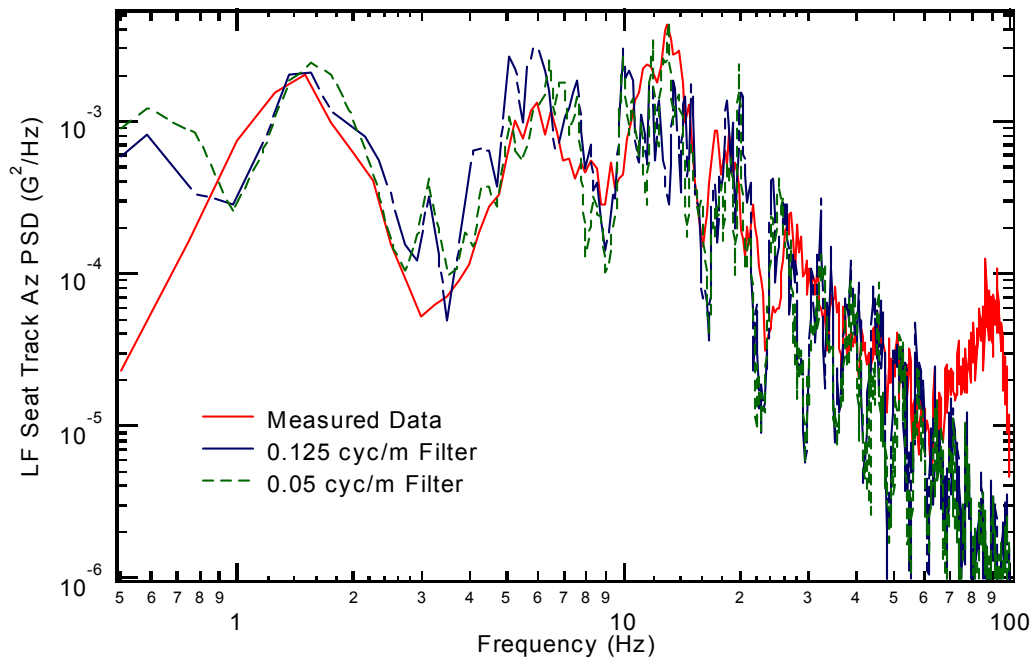


Figure 14: Comparison of vehicle model seat track vibration with the field measurement.

First, as expected, Figure 14 shows that the vehicle response has higher amplitude on this road surface than that caused by the smooth road. The PSD peaks at about $4 \times 10^{-3} \text{ G}^2/\text{Hz}$ (Figure 14) compared to $1 \times 10^{-4} \text{ G}^2/\text{Hz}$ for the smooth road surface (Figure 9). Second, the low resonance frequency near 0.6 Hz of the model prediction is most likely the result of incomplete removal of the instrumental drift. This response is not observed in the vehicle data. Third, the 0.05 cyc-m^{-1} high pass filter correlated better with the test data than that of the 0.125 m^{-1} filter for the region from 3 to 12 Hz. This suggests that a better profile was generated with the 0.05 cyc-m^{-1} high pass filter for the road surface. This might also give some insight for the deviation in comparison in smooth road as shown in Figure 8 from 3.5 to 6 Hz range (Figure 9). It is more likely that the filter used did not remove some drifts in the road data which caused the resonance as shown in Figure 8. Fourth, the resonance at about 90 Hz of the test data is consistent with the smooth road test results as shown in Figure 9. This is the tire second vertical vibration mode. The single

spring tire model used in the simulations does not include this mode [6] and hence is not possible for the model to reproduce the resonance near 90Hz. It is believed that the inclusion of the tire second vertical mode should improve further the analysis predictions. Finally, we notice that the correlation of simulations with measured data is better for the rough road for frequency higher than 20 Hz than that of the smooth road as shown in Figure 9.

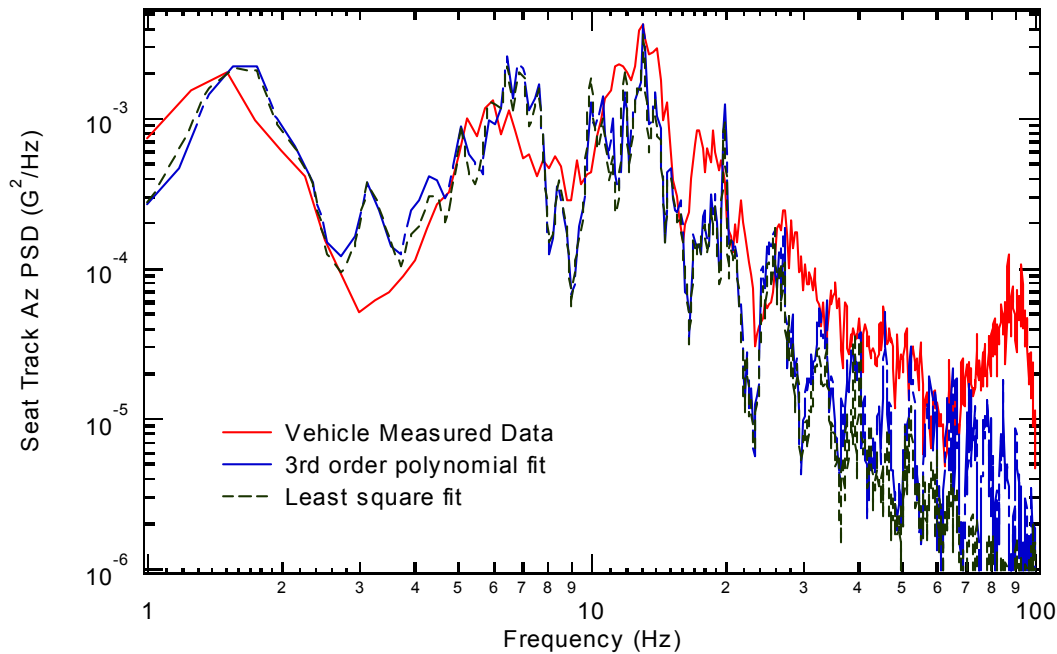


Figure 15: Comparison of road profile modeling techniques. Fitted curve yields better correlation for higher frequencies.

As was done for the smooth road, the road profile sampling distance at 150mm is also studied with different modeling techniques and is shown in Figure 15. The least square average method clearly shows a tendency of under-predicting the vehicle resonance because of the reduced sampling points. Thus, it is lower than the results using finer resolution as it was shown in Figure 14. Less road information yields less accurate vehicle response is reasonable. However, the use of the four point 3rd order polynomial fit increased the road profile information, especially the normal direction, and hence the resonance for higher frequencies are brought up slightly almost similar to the use of the 5mm sampling distance data. In combining with the observation in the smooth road surface simulations, the 4 point polynomial fitted road surface should be used for the road profile data measured at 6 inches interval.

CONCLUSIONS

Based on the study reported in this paper we conclude the following:

1. The higher accuracy road profile can improve the vehicle model resonance predictions.
2. If the road profile resolution is substantially less than half of the tire patch length, the least square averaging method is sufficient for calculating the ground height and normal direction for driving simulation input.

3. When the road sampling distance is close to or greater than the tire patch length a third order polynomial fit to the 4 nearest points of the tire contact point should be used to approximate the road surface height and normal direction. It yields better vehicle resonance responses.
4. To increase the model predictions to higher confidence level requires an improved tire model that includes the second vertical tire vibration mode.

REFERENCES

1. Kao, Ben G., *A Three-Dimensional Dynamic Tire Model for Vehicle Dynamic Simulations*, **Tire Science and Technology**, TSTCA, Vol. 28, 2000, pp. 72-95. Also in **The Annual Review of Tire Materials and Tire Manufacturing Technology**, **Tire Technology 2000**, UK and International Press, August 2000, pp. 10-17.
2. Turpin, Darrell R., Application of High-Fidelity Surface Tire Force Models In Real-Time Simulation, Proceedings of Driving Simulation Conference, Sophia Antipolis, France, September 12-13, 1995, TEKNEA, Toulouse, 1995.
3. Greenberg, J. A. and T. J. Park, "The Ford Driving Simulator", SAE Paper Number 940176, SAE International Congress and Exposition, Detroit, Michigan, 1994.
4. Kao, Ben G., Ronald H. Miller, Jeffry A. Greenberg and Gary S. Strumolo, High Performance Computing: A Mathematical Aerodynamic Model for Vehicle Driving Simulations, Editor: T. I. O'Hern: FED-Vol. 253, Proceedings of the ASME, Fluids Engineering Division, Book No. H01212 - 2000, pp. 335-344.
5. Bakker, E., H. B. Pacejka and L. Lidner, *A New Tire Model with an Application in Vehicle Dynamics Studies*, SAE Paper No. 890087, 4th Autotechnologies Conference, Monte Carlo, January 1989.
6. Kao, Ben G., *Tire Vibration Modes and Tire Stiffness*, Presented to the 20th Annual Conference of the Tire Society, April 24, 2001.
7. Vehicle Dynamics Committee, *Vehicle Dynamics Terminology - SAE Recommended Practice*, SAE J670e, July 1976.